Author Manuscript

Author Manuscript

Author Manuscript

Author Manuscript

HHS Public Access

Author manuscript

Mech Dev. Author manuscript; available in PMC 2020 February 01.

Published in final edited form as:

Mech Dev. 2019 February ; 155: 15–26. doi:10.1016/j.mod.2018.10.002.

Non-obstructive vas deferens and epididymis loss in cystic fibrosis rats

Z.E. Plyler[1], **S.E. Birket**[2], **B.D. Schultz**[3], **J. S. Hong**[4], **S.M. Rowe**[2], **C.F. Petty**[2], **M.R. Crowley**[5], **D.K. Crossman**[5], **T.R. Schoeb**[5], and **E.J. Sorscher**[4,*]

[1]Department of Biology, University of Alabama at Birmingham, Birmingham, AL, USA

[2]Division of Pulmonary, Allergy and Critical Care Medicine, University of Alabama at Birmingham, Birmingham, AL, USA

[3]Department of Anatomy & Physiology, Kansas State University College of Veterinary Medicine, Manhattan, KS, USA

[4]Department of Pediatrics, Emory University School of Medicine, Atlanta, GA, USA

[5]Department of Genetics, University of Alabama at Birmingham, Birmingham, AL, USA

Abstract

This study utilizes morphological and mechanistic endpoints to characterize the onset of bilateral atresia of the vas deferens in a recently derived cystic fibrosis (CF) rat model. Embryonic reproductive structures, including Wolffian (mesonephric) duct, Mullerian (paramesonephric) duct, mesonephric tubules, and gonad, were shown to mature normally through late embryogenesis, with involution of the vas deferens and/or epididymis typically occurring between birth and postnatal day 4 (P4), although timing and degree of atresia varied. No evidence of mucus obstruction, which is associated with pathology in other CF-affected tissues, was observed at any embryological or postnatal time point. Reduced epididymal coiling was noted post-partum and appeared to coincide with, or predate, loss of more distal vas deferens structure. Remarkably, α smooth muscle actin expression in cells surrounding duct epithelia was markedly diminished in CF animals by P2.5 when compared to wild type counterparts, indicating reduced muscle development. RNA-seq and immunohistochemical analysis of affected tissues showed disruption of developmental signaling by Wnt and related pathways. The findings have relevance to vas deferens loss in humans with CF, where timing of ductular damage is not well characterized and underlying mechanisms are not understood. If vas deferens atresia in humans begins in late gestation and continues through early postnatal life, emerging modulator therapies given perinatally might preserve and enhance integrity of the reproductive tract, which is otherwise absent or deficient in 97% of males with cystic fibrosis.

[*]Corresponding Author: Eric J. Sorscher, M.D., Emory University, 1760 Haygood Drive, Suite 280, Atlanta, GA 30322. Phone: (404) 727-3293., esorscher@emory.edu.

Author Manuscript Author Manuscript Author Manuscript Author Manuscript

Introduction

The cystic fibrosis transmembrane conductance regulator (CFTR) −/− rat exhibits numerous tissue abnormalities similar to those observed in human CF patients, including pulmonary remodeling, loss of gastrointestinal tissue integrity, secretory/exocrine dysfunction, osteopenia, and bone and dental defects[1]. Male CF rats also exhibit bilateral absence of the vas deferens. Greater than 97% of human subjects harboring mutations on both CFTR alleles exhibit an absent or atretic vas deferens, and carriers of CFTR variants are predisposed to congenital bilateral absence of the vas deferens (CBAVD), a condition leading to infertility and considered a mild form of CF[2].

Analysis of male reproductive ducts in larger CF animal models such as pigs[3,4] and ferrets[5] has demonstrated more dramatic genitourinary abnormalities than have been observed in murine models[6,7], although the onset of observable differences has not been determined in any species. The CF rat offers an opportunity to characterize timing, extent, and signaling pathways that underlie dysgenesis or atresia of the vas deferens and associated epididymal structures. In the present study, timed matings of heterozygous animals were used to monitor genitourinary tissue between embryonic day 15.5 (E15.5; 15 days post conception) and postnatal day 8 (P8), as part of a more comprehensive evaluation to determine onset and possible mechanisms contributing to vas deferens atresia.

Methods and Materials

Animals and husbandry.

Protocols involving animals were reviewed and approved by the University of Alabama at Birmingham animal care and use committee and performed in accordance with established guidelines[8]. All animals received standard housing, nutrition, water, and light/dark cycle care, as described previously[1]. Female CFTR +/− animals were paired for breeding and monitored daily for evidence of vaginal plugging. Females with a vaginal plug were separated and weighed at least three times each week to confirm pregnancy and monitor progress of gestation.

To obtain prenatal samples, pregnant females at desired time points (i.e. days post conception) were euthanized using CO_2 inhalation, followed by cervical dislocation and dissection to retrieve fetal tissue. Neonatal rats were sacrificed by decapitation. Animals were genotyped for CFTR expression by PCR as reported previously[1].

Tissue processing and histology.

Fetal and postnatal tissues were submerged and fixed in alcoholic formalin (buffered 70% ethanol in water, 10% formalin; Fisher Scientific, Bridgewater, NJ, USA), in water) at room temperature (22° C) immediately following dissection. Samples were then embedded in paraffin by dehydration with increasing ethanol concentrations (70%, one hour; 95%, one hour; 100% twice at one hour each), clearing with 100% xylene (two incubations at 1 hour each) and two heated paraffin treatments (1 hour each), followed by block embedding in paraffin. Tissues prepared in this manner were sectioned by microtome at 5 μm and mounted on glass slides. Resulting samples were deparaffinized and stained with hematoxylin and

Author Manuscript Author Manuscript Author Manuscript Author Manuscript

eosin (H&E) or Alcian blue periodic acid Schiff (AB-PAS)[9]. Images were captured using EVOS XL Core (ThermoFisher Scientific, Waltham, MA, USA).

Immunohistochemistry and TUNEL assays.

In tissue sections prepared as above, antigens were accessed by heating in citrate solution (Fisher Scientific; pH 6; 95° C for 20 minutes), followed by cooling to room temperature. Three percent hydrogen peroxide and PBS (GIBCO BRL, Grand Island, NY, USA) with Tween 20, 5% bovine serum albumin/2% goat serum (Zymed, South San Francisco, CA, USA; 'blocking solution') were used to occlude endogenous peroxidases and nonspecific protein binding sites. Primary antibodies diluted in blocking solution were incubated with tissue sections overnight in a humidified chamber at 4° C. Following additional washing and blocking steps (blocking solution), samples were incubated with horseradish peroxidase (HRP)-conjugated secondary antibody (e.g., goat anti-rabbit or goat anti-mouse) in blocking solution for 1.5 hours. Samples were then washed and exposed to 3,3′-diaminobenzidine (DAB) solution for 3–20 minutes to allow sufficient pigment deposition for detection by microscopy (with counterstaining by hematoxylin for 10 seconds). Primary antibodies directed against TGFβ1 (cat #sc-146, Santa Cruz Biotechnology, Dallas, TX, USA; 1:500 in blocking solution), pSmad2/3 (cat #8828, Cell Signaling Technology, Danvers, MA, USA; 1:500), α-actin (cat #sc32251, Santa Cruz; 1:500), Wnt9b (LifeSpan BioSciences, Seattle, WA, USA; A9079; 1:500), androgen receptor (Abcam, Cambridge, MA, USA; ab3510; 1:500), and phopho-androgen receptor (Abcam ab45089; 1:500) were used to monitor protein expression in the region of the vas deferens. Studies without primary antibodies were evaluated in parallel in all cases. For the TUNEL assay, a commercially available in situ apoptosis detection kit (TumorTACS™, Trevigen, Inc. Gaithersburg, MD, USA) was employed according to manufacturers' protocol.

Image processing, stacking, and three-dimensional rendering in two-dimensions.

Images were loaded using pre-compiled open source Fiji ImageJ software (http://fiji.sc/Downloads#Fiji) to sharpen/optimize image contrast ("Enhance Contrast" function). For regions with intact sequential sections, data were configured as a stack and rotated/aligned using the "Registration" plug-in and "Stackreg" function. Z-Project was then applied to each sequence montage to generate images displaying: i) transparent overlay of the stack ("Sum Slices" projection type), and ii) color coded standard deviation ("Standard Deviation" type). The "Sum Slice" output images for multiple stacks were compiled into secondary files, with Z-Project again used to generate 3-dimensional images in 2-dimensions (each representing 10 sections (i.e., 50 μm depth)). To measure optical density for analysis of cellularity, images were converted to 8-bit format and set at standard threshold. For each slide used, three to four duct cross-sections were chosen randomly and optical density measured within a region of interest (ROI) immediately external to the epithelia structure. Using appropriately scaled conversion (pixels per μm; derived from scale bar generated by the imager), the area (A) of each cross-sectional lumen was determined with ImageJ, and lumenal diameter (d) calculated as $d=2(\sqrt{A}/\pi)$.

Author Manuscript Author Manuscript Author Manuscript Author Manuscript

RNAseq and analysis.

RNA was isolated from regions of the microdissected male reproductive cord (comprised of epithelia, smooth muscle, and mesenchyme) using a commercially available kit (RNeasy, Qiagen, Venlo, The Netherlands). A sequence library was established using 100 μg of RNA (Sure Select RNA Stranded Kit, Agilent, Santa Clara, CA, USA). RNA-seq libraries were evaluated using HiSeq 2500 equipment (Illumina, San Diego, CA, USA) and reads mapped with Tophat[10,11] Quantification (raw counts and fragments per kilobase of transcript per million (FPKM)) of mapped reads were determined using Cuffcompare or Cuffdif[12].

Statistical analysis.

Data were summarized as mean ± SEM. Two-tailed *t* tests were used to assess statistical significance of observed differences in staining density across two conditions applied to a particular time point or sample. *P* values of less than 0.05 were considered significant. For RNA-seq analysis and comparisons among fragments per kilobase transcript per million, TopHat version 2.1.1 was used to align raw RNA-Seq fastq reads to the USCS rat reference genome (rn5) using the short read aligner Bowtie 2.3.3.1[12–14]. Cufflinks version 2.2.1 used the aligned reads from TopHat to assemble transcripts, estimate their abundance and test for differential expression and regulation[11,12]. Associated Cuffdiff software was used for assessing significant changes in transcript expression, splicing and promoter use. When genes with statistically significant changes in absolute expression were evaluated, a t-test (as above) was used to calculate p values of the observed values.

Results

Embryonic Wolffian ducts develop normally in CFTR−/− male rat embryos.

Testosterone production begins at approximately E15.5 in the male rat fetus and is believed to stabilize the Wolffian duct by inhibiting its involution. A perinatal testosterone surge may also activate fluid and electrolyte transport through CFTR in tissues such as the vas deferens[15–16] (see also below). In female rats, onset of Wolffian duct involution becomes apparent by E17.5-E18.5[17–19]. Studies were therefore established to determine whether: 1) detectable differences in Wolffian duct development, relative to CFTR +/+ littermates (referred to as wild type for purposes of this report), could be observed in E15.5 CFTR −/− males (i.e., at a time prior to androgen stabilization); 2) mucus secretion, accumulation or obstruction (an explanation often proposed to account for vas deferens atresia in CF patients) is observed in fetal or neonatal reproductive ducts of animals lacking CFTR expression; 3) CFTR−/− Wolffian structures at E17.5 exhibit features consistent with ablated androgen signaling; and 4) CFTR−/− male rats are born with patent excurrent reproductive ducts. As shown in Figure 1, Wolffian ducts (W) of E15.5 CFTR−/− rats (Panel A, g-l) are intact with no apparent differences from their wild type counterparts (Panel A, a-f). Clear and obvious Wolffian duct lumina are observed in all samples. Mullerian ducts were observed in all E15.5 fetuses, with evidence of Mullerian duct regression observed at this timepoint in a CFTR−/− animal (Panel A, k, l). In E17.5 fetuses, Wolffian ducts again were prominent and not discernibly different in CFTR−/− tissues (Panel B, f-i) when compared to wild type (Panel B, a-d). Mullerian ducts were less prominent or not observed at E17.5, again with no detectable difference between wild type and CFTR−/− fetuses. Patency was

Author Manuscript Author Manuscript Author Manuscript Author Manuscript

noted at all locations along the full length of both the CF and non-CF Wolffian duct at E15.5 and E17.5, including regions adjacent to the gonad (Panel B; a,c,f,h) and more caudal areas near the developing prostate (b,d,g,i). Importantly, AB-PAS staining provided no evidence of mucus accumulation or obstruction in any of the animals examined.

Dramatic loss of epididymal integrity and ductular maturation in perinatal CFTR−/− rat.

Although embryonic Wolffian duct development appears normal at E15.5 and E17.5, the situation is significantly different at birth. Figure 2 shows reproductive tract phenotype observed at P0.5. Four of six CFTR−/− males demonstrated features of epididymal underdevelopment, including diminished mesenchymal cell density immediately surrounding the epithelium, an observation that suggests dysgenesis of periductular smooth muscle (compare regions just exterior to the dashed circles in Figure 2A, a and c). Periductular cellularity is quantified and compared directly in panel B. Reduced lumen diameter of corpus epididymis was also noted and compared in panel C. In these instances, the epididymis showed histological evidence for convoluted epithelial structures—although a clearly defined lumen could not always be detected i.e., apical aspects of opposing epithelial cells were in virtual contact (described further below). In all CFTR−/− animals at birth, a widely patent vas deferens could be observed in at least a portion of the duct (Figure 2A, panel d), which appeared comparable to CFTR+/+ vas deferens (panel b). However, serial sections taken across 30–60 μm showed vas deferens narrowing to the point that no lumen could be discerned in many animals (Figure 3). These and additional sequential sections showed loss of typical epithelial morphology and absence of cells with epithelioid characteristics, In some cases, the CFTR−/− proximal vas deferens appeared slightly dilated when compared to wild type (see Figure 2, compare images b and d).

All CFTR−/− male rats exhibited gross abnormalities of their reproductive tracts at all time points beyond P0.5, with complete loss of the vas deferens as animals mature (Supplemental Figure 1). As shown in Figure 4, P1.5 CFTR−/− animals exhibit markedly underdeveloped reproductive structures, including reduced coiling of epididymal ducts, as evidenced by fewer duct cross-sections, and diminished surrounding mesenchymal cellularity compared to CFTR+/+ tissues. Epididymis, particularly the corpus, showed ductal collapse in most CFTR −/− animals, similar to that observed in the vas deferens at P0.5 (Figure 3). Serial sectioning/ stacking of images further establish reduced epididymal development and diminished surrounding smooth muscle wall (Figure 5A and 5B), together with reduced lumenal diameter (Figure 5C). Again, no signs of mucus obstruction or plugging were observed in any sections from any animals.

Similar defects, including collapsed epididymis and vas deferens, together with reduced mesenchyme and smooth muscle were noted in animals at subsequent time points. For example, Figure 6 provides representative images from animals studied at P2.5. Note that CFTR−/− rats demonstrate poorly developed epididymal structure with relative absence of surrounding smooth muscle (b-d,f), and lumenal collapse to a point where ductular epithelium is no longer distinguishable (particularly in the corpus epididymis, compare image b to d). As with earlier time points, segments of the vas deferens were patent with smooth muscle evident (m), whereas collapse and failure of duct maturation was observed in

Author Manuscript Author Manuscript Author Manuscript Author Manuscript

distal sections (n). Other animals exhibited severely collapsed and/or degenerate vas deferens (j-l; compare to CFTR+/+, g-i). In specific cases at P2.5, only a remnant of the CFTR−/− vas deferens (with no apparent smooth muscle development) could be seen (k). The findings suggest an abnormal transition of ductular structures, with loss of epithelial organization.

Diminished smooth muscle surrounding CFTR−/− reproductive tract structures accompanies loss of ductal integrity.

Elevated myofibroblast proliferation has been noted in CF lung and other tissues, and is believed to mediate damage through TGFβ dependent activation and signaling[20]. No indication of elevated TGFβ/pSMAD signaling in the region of CFTR−/− rat vas deferens—and no evidence of myofibroblast proliferation—were noted (not shown). In contrast, a profound decrease in α-SMA immunoreactivity was observed in the region immediately surrounding epithelial cells in CFTR−/− ducts, indicating reduced smooth muscle differentiation (Figure 7A). A 'corona' of α smooth muscle actin immunoreactivity at P2.5 was both broader and more intense in epididymis from CFTR+/+ compared to corresponding CFTR−/− tissues. Scoring chromogen intensity confirmed reduction of α-SMA immunoreactivity in CFTR−/− tissues at this time point (Figure 7B). Importantly, no detectable expression of α-SMA was associated with either CFTR+/+ or CFTR−/− reproductive ducts late in fetal development (E17.5, Figure 7C), when duct formation appeared normal despite the absence of CFTR. α smooth muscle actin expression in other organs such a bladder (not shown) or colon (Figure 7C) did not appear compromised by absence of CFTR.

RNAseq analysis of male reproductive cord indicates altered Wnt and androgen signaling.

An RNA expression profile was constructed for CFTR−/− reproductive cord at birth (i.e., a timepoint when dysgenesis of epididymis and vas deferens becomes apparent). Messenger RNA was isolated from tissues, including epididymis, vas deferens, and surrounding mesenchyme, which were isolated from newborn CFTR+/+ and CFTR−/− pups. RNA-seq from two independent litters revealed 72 transcripts significantly over- or under-expressed (Supplemental Table 1). Average fragment per kilobase transcript per million reads (FPKM) values for the 14 most significantly up- or down-regulated transcripts are shown in Figure 8. Enriched gene ontology (GO) terms generated for differentially expressed mRNAs using PANTHER for biological process, molecular function, and related pathways are also shown (Table 1 and Supplemental Table 2). Notable ontologies identified here include processes that govern tissue and organ development (including muscle), transcription factor activity, and Wnt signaling.

Wnt9b is known to play an important role during tubulogenesis in numerous tissues, and mice lacking this protein exhibit loss of the epididymis, similar to our findings for CFTR−/− rats[21]. To confirm RNAseq results, immunolabeling of tissue sections from each region of the developing epididymis and vas deferens was performed (Figure 9). Labeling of Wnt9b was most intense in corpus epididymis duct epithelium, as well as developing smooth muscle of CFTR+/+ animals. Although less intense, epithelia in the caput and cauda epididymis also provided a signal indicative of Wnt9b expression. In contrast, a weak signal

Author Manuscript Author Manuscript Author Manuscript Author Manuscript

for Wnt9b expression was observed in corpus epididymis epithelial cells of CFTR−/− animals with no clear signal in the surrounding region (i.e., developing muscle). Moreover, no detectable Wnt9b signal was observed in either caput or cauda epididymis from CFTR−/− animals. Androgen signaling is also known to play a role during reproductive tract maturation by: 1) stabilizing the mesonephric duct during early embryogenesis and 2) conferring maturation of the reproductive duct peri- and post-natally. Immunohistochemistry of total and activated androgen receptor suggested lower androgen signaling activity in CFTR−/− animals compared to wild type (Figure 10).

TUNEL assay to evaluate apoptosis in the CF reproductive tract.

To investigate whether programmed cell death contributes to involution of reproductive duct in CFTR −/− animals, terminal deoxynucleotidyl transferase (TdT) dUTP Nick-End Labeling (TUNEL) assays were conducted on samples taken just following birth. Representative cross-sections are shown in Supplemental Figure 2, together with positive (nuclease treated) and negative (no primary antibody) controls. While some regions of the CF reproductive tract exhibit slightly positive staining in ductal epithelia, the findings do not indicate apoptosis as a primary determinant of CFTR−/− reproductive tract abnormalities.

Discussion

Loss of the vas deferens affects >97% of CF male patients, and in rare cases ductular atresia may be the only manifestation of a deleterious CFTR variant. Males with evidence of congenital bilateral absence of the vas deferens who are otherwise healthy are often found to carry mild cystic fibrosis-associated mutations[22–25]. The mechanism that underlies CFTR dependent involution of the male reproductive tract is not known. A traditional hypothesis suggests that mucus obstruction in the developing vas deferens—in semblance to other CF-affected tissues such as lung, liver, and pancreas—might elicit tissue injury, fibrosis, and general atresia[26]. In the present study, no evidence of mucus obstruction in the rat CF epididymis or vas deferens was found at any time point in any of the animals evaluated.

A similar observation has been made previously in CF pig, although limited information regarding this point is available from human studies[3,27]. Our findings indicate that embryonic structures including the mesonephric (Wolffian) and paramesonephric (Mullerian) ducts develop normally in CF animals. In contrast, dysgenesis and involution of the CF epididymis and vas deferens were noted to occur perinatally. During the postnatal period, most CF animals showed underdevelopment of smooth muscle surrounding the ductular structures, diminished epithelial proliferation, reduced epididymal coiling and maturation, and regional collapse of the vas. By the third day of life, the vas deferens was essentially absent, although remnants were occasionally observed as late as 8 days postnatal. These findings indicate that the disease designation “congenital bilateral absence of the vas deferens” may represent a misnomer. Perhaps “bilateral atresia of the epididymis and vas deferens” would be more appropriate.

Normal male reproductive tract development comprises multiple stages, each with crucial windows for maturation of the mesonephros. The duct serves an excretory function for embryonic kidney, and many of the same pathways that govern renal development may also

Author Manuscript Author Manuscript Author Manuscript Author Manuscript

influence mesonephric integrity. Tubular development in some settings may be linked to a CFTR protein interaction with the ZO-1—ZONAB dependent pathway[28]. Signaling mechanisms shown previously to impact male reproductive anatomy include homeobox (HOX) and HOX-like transcription factors and target genes, several growth factors, and WNT-dependent signaling pathways, among others[17–19, 29–31]. Notably, WNT9B knockout mice have been shown previously to exhibit complete loss of the epididymis[21].

RNA-seq analyses from wild-type and CF animals at birth (using samples obtained from reproductive cord epithelia, smooth muscle, and mesenchyme), were used to investigate potential genes and pathways contributing to vas deferens atresia. Ontological studies revealed striking abnormalities of genes involved in developmental processes responsible for muscle, ectoderm, renal and mesonephric development. Most notably, pronounced changes in Wnt signaling were observed. For example, Wnt9b was found to be >36 fold under-expressed in reproductive cord of CFTR−/− rat newborns, a finding confirmed by immunohistochemistry.

Myogenin (MYOG) was over-expressed in CF rat reproductive cord. This gene product has been linked to Wnt-signaling, including a role during muscle cell differentiation and/or development[32]. Normal levels of androgen receptor protein expression were noted in epithelial cells lining the epididymis, with modestly decreased phosphorylation of the receptor at positions S210 and S215. CFTR fluid and electrolyte secretion are activated by androgen stiumulation in genitourinary epithelium through a prostaglandin dependent pathway[15,16,33]. Moreover, prostaglandins in this setting may be metabolized in a manner that is influenced by local bicarbonate concentrations regulated by CFTR. Future studies will therefore be necessary to investigate a potential relationship between androgen stimulation, CFTR function, and loss of the vas deferens in CF or CBAVD. SP5, a transcription factor known to impact Wnt expression[34,35], was under-expressed by >12 fold in CF samples. Other under-expressed transcripts include the GATA3 homeobox containing transcription factor, deletion of which in mice leads to dysgenesis and regression of the Wolffian duct in mid- to late gestation. Interestingly, the most markedly under-expressed transcript was miR290, a microRNA shown to influence stem cell levels and pluripotency during development[36].

Several recent reports have described developmental features responsible for elongation and coiling of the epididymis[17–19, 29–31]. In one study, physical resistance to epithelial expansion due to developing smooth muscle was shown to regulate maturation of epididymal tissues[37]. The present report demonstrates lack of smooth muscle in the CFTR−/− male reproductive tract, a finding that could contribute to ductular dysmorphology. A relationship of these observations to recent data concerning CFTR expression in mouse, rat, and porcine smooth muscle (within lung and intestinal tissues) remains to be determined[38–40].

Based on mechanistic evaluation of tissue damage in the CF lung and pancreas, an emerging hypothesis for generalized CF exocrine destruction involves defective epithelial-mesenchymal transition (EMT) associated with increased TFGβ1, enhanced pSMAD signaling, and accompanying myofibroblast proliferation[20]. TFGβ1 is an established genetic modifier of CF respiratory decline[20, 41–46]. Our results, however, do not suggest increased

Author Manuscript Author Manuscript Author Manuscript Author Manuscript

TGFβ1 signaling through pSMAD2/3 in reproductive tissues of CFTR−/− animals (Supplemental Figure 3). In contrast to other CF organs, α-SMA staining indicative of smooth muscle development is decreased (rather than increased) in the perinatal reproductive tract of CFTR null rats. Our results also fail to implicate apoptosis during involution of CF male reproductive anatomy. On the other hand, there is growing evidence that tissue damage in cystic fibrosis may be attributable to defects of key tissue repair pathways governed by pH, local chloride concentration, or other abnormalities mediated by CFTR dependent anion (including bicarbonate) transport[47–50]. Mechanisms such as these may provide a link between CFTR activity and vas deferens ablation in the cystic fibrosis rat model.

In summary, CFTR−/− male rats are often born with a degenerating vas deferens and significant epididymal under-development. The observations of abnormal epididymis and no evidence of mucus plugging are consistent with findings in newborn CF piglets, and suggest a common pathogenic mechanism for the phenotype described here[3]. Our results establish that loss of smooth muscle surrounding the reproductive tract accompanies disruption of ductular anatomy, as reflected by diminished α smooth muscle actin and an atretic smooth muscle wall. RNA-seq and immunohistochemistry indicate participation of Wnt9b signaling (together with other important upstream transcription factors) during involution of the CF vas deferens.

The present study suggests a means by which vas deferens atresia and CFTR-dependent abnormalities of tissue architecture, remodeling, and infertility can be better understood. In particular, observation of peri- or postnatal loss of the vas deferens in CF animals indicates importance of determining whether human males with CF retain a functional duct structure immediately after birth. While it is clear that progressive damage to numerous tissues (pancreas, lung, liver) occurs among CF patients throughout their lifespan, timing of vas deferens destruction in man has not been well characterized. Our results indicate the potential for emerging CFTR-based modulator therapies—administered during critical periods of prenatal or postnatal life—as a means to conserve integrity of the male reproductive tract in subjects with the disease. In this context, a new CF rat model encoding ivacaftor-responsive humanized G551D CFTR has recently been completed by our laboratory using gene editing technology and—based on findings presented here—should allow pharmacologic rescue of CF genitourinary defects to be more thoroughly evaluated in the future.

Supplementary Material

Refer to Web version on PubMed Central for supplementary material.

Acknowledgements:

Funding for this project was provided by CFF SORSCH R464 and NIH P30 DK072482. This manuscript also represents contribution number 18–606-J from the Kansas Agricultural Experiment Station.

Author Manuscript Author Manuscript Author Manuscript Author Manuscript

References

1. Tuggle KL, Birket SE, Cui X, et al. Characterization of defects in ion transport and tissue development in Cystic Fibrosis Transmembrane Conductance Regulator (CFTR)-knockout rats. PLoS One 2014; 9(3):e91253/journal.pone.00921253. doi: 10.1371/journal.pone.0091253..
2. Grangeia A, Sa R, Carvalho F, et al. Molecular characterization of the cystic fibrosis transmembrane conductance regulator gene in congenital absence of the vas deferens. Genet Med 2007; 9(3):163–172. doi:10.1097GIM.0b013e3180318aafyi. [PubMed: 17413420]
3. Pierucci-Alves F, Akoyev V, Stewart JC, et al. Swine models of cystic fibrosis reveal male reproductive tract phenotype at birth. Biol Reprod 2011; 85(3):442–451. doi: 10.1095/biolreprod.111.090860. [PubMed: 21593481]
4. Yi S, Pierucci-Alves F, Schultz BD. Transforming growth factor-β1 impairs CFTR-mediated anion secretion across cultured porcine vas deferens epithelial monolayer via the p38 MAPK pathway. Am J Physiol Cell Physiol 2013; 305(8):C867–C876. doi: 10.1152/ajpcell.00121.2013. [PubMed: 23903699]
5. Sun X, Sui H, Fisher JT, et al. Disease phenotype of a ferret CFTR-knockout model of cystic fibrosis. J Clin Invest 2010; 120:3149–3160. doi: 10.1172/JCI43052. [PubMed: 20739752]
6. Reynaert I, Van Der Schueren B, Degeest G, et al. Morphological changes in the vas deferens and expression of the cystic fibrosis transmembrane conductance regulator (CFTR) in control, deltaF508 and knock-out CFTR mice during postnatal life. Mol Reprod Dev 2000; 55:125–135. doi: 10.1002/(SICI)1098-2795(200002)55:2<125::AID-MRD1>3.0.CO;2-Q [PubMed: 10618651]
7. Durie PR, Kent G, Phillips MJ, et al. Characteristic multiorgan pathology of cystic fibrosis in a long-living cystic fibrosis transmembrane regulator knockout murine model. Am J Pathol 2004;164(4):1481–93. doi: 10.1016/S0002-9440(10)63234-8 [PubMed: 15039235]
8. Guide for the care and use of laboratory animals. Eighth Edition Committee for the Update of the Guide for the Care and Use of Laboratory Animals. The National Academies Press, Washington, D.C 2011.
9. Humason G Animal tissue techniques. San Francisco, W.H. Freeman 1962.
10. Kim D, Pertea G, Trapnell C, et al. TopHat2: accurate alignment of transcriptomes in the presence of insertions, deletions and gene fusions. Genome Biol 2013; 14(4):R36. doi: 10.1186/gb-2013-14-4-r36. [PubMed: 23618408]
11. Trapnell C, Williams BA, Pertea G, et al. Transcript assembly and abundance estimation from RNA-Seq reveals thousands of new transcripts and switching among isoforms. Nature Biotechnol 2010; 28(5):511–15. doi: 10.1038/nbt.1621. [PubMed: 20436464]
12. Trapnell C, Hendrickson DG, Sauvageau M, et al. Differential gene and transcript expression analysis of RNA-seq experiments with TopHat and Cufflinks. Nat. Protocols 2012;7(3):562–578. doi: 10.1038/nbt.2450. [PubMed: 22383036]
13. Trapnell C, Pachter L, Salzberg SL. TopHat: discovering splice junctions with RNA-Seq. Bioinformatics 2009; 25(9):1105–11. doi: 10.1093/bioinformatics/btp120. [PubMed: 19289445]
14. Langmead B, Trapnell C, Pop M, Salzberg SL. Ultrafast and memory-efficient alignment of short DNA sequences to the human genome. Genome Biol 2009; 10(3):R25. doi: 10.1186/gb-2009-10-3-r25. [PubMed: 19261174]
15. McKanna JA, Zhang MZ, Wang JL, et al. Constitutive expression of cyclooxygenase-2 in rat vas deferens. Am J Physiol 1998; 275(1 Pt2): R227–233. [PubMed: 9688983]
16. Pierucci-Alves F, Duncan CL, Schultz BD. Testosterone upregulates anion secretion across porcine vas deferens epithelia in vitro. Biol Reprod 2009; 81(4): 628–635. doi: 10.1095/biolreprod.109.076570. [PubMed: 19474062]
17. Joseph A, Yao H, Hinton BT. Development and morphogenesis of the Wolffian/Epididymal Duct, More Twists and Turns. Dev Biol 2009; 325(1):6–14. doi: 10.1016/j.ydbio.2008.10.012. [PubMed: 18992735]
18. Barsoum I, Yao HH-C. The road to maleness: from testis to Wolffian duct. Trends Endocrinol Metab 2006; 17(6):223–228. doi: 10.1016/j.tem.2006.06.009 [PubMed: 16822678]
19. Jirsova Z, Vernerova Z. Involution of the Wolffian duct in the rat. Funct Dev Morphol. 1993; 3(3):205–6. [PubMed: 8167402]

Author Manuscript Author Manuscript Author Manuscript Author Manuscript

20. Harris WT, Kelly DR, Zhou Y, et al. Myofibroblast Differentiation and Enhanced Tgf-B Signaling in Cystic Fibrosis Lung Disease. Morty RE, ed. PLoS One 2013;8(8):e70196. doi: 10.1371/journal.pone.0070196. [PubMed: 23950911]
21. Carroll TJ, Park JS, Hayashi S, et al. Wnt9b plays a central role in the regulation of mesenchymal to epithelial transitions underlying organogenesis of the mammalian urogenital system. Dev Cell 2005; 9: 283–292. doi: 10.1016/j.devcel.2005.05.016 [PubMed: 16054034]
22. Anguiano A, Oates RD, Amos JA, et al. Congenital bilateral absence of the vas deferens. A primarily genital form of cystic fibrosis. JAMA 267: 1794–1797, 1992. [PubMed: 1545465]
23. Cuppens H, Cassiman JJ. CFTR mutations and polymorphisms in male infertility. Int J Androl 2004; 27(5): 251–6. doi: 10.1111/j.1365-2605.2004.00485.x [PubMed: 15379964]
24. Gallati S, Hess S, Galie-Wunder D, et al. Cystic fibrosis transmembrane conductance regulator mutations in azoospermic and oligospermic men and their partners. Reprod Biomed Online 2009; 19(5):685–94. [PubMed: 20021716]
25. Blau H, Freud E, Mussaffi H, et al. Urogenital abnormalities in male children with cystic fibrosis. Arch Dis Child 2002; 87(2):135–138. [PubMed: 12138064]
26. Oppenheimer EH, Esterly JR. Observations on cystic fibrosis of the pancreas. V. Developmental changes in the male genital system. J Pediatr 1969; 75(5):806–811. [PubMed: 5357932]
27. Gaillard DA, Carré-Pigeon F, Lallemand A. Normal vas deferens in fetuses with cystic fibrosis. J Urol 1997; 158(4):1549–1552. [PubMed: 9302172]
28. Ruan YC, Wang Y, Da Silva N, et al. CFTR interacts with ZO-1 to regulate tight junction assembly and epithelial differentiation through the ZONAB pathway. J Cell Sci 2014; 127(20):4396–4408. doi:10.1232/jcs.148098. [PubMed: 25107366]
29. Shaw G, Renfree MB. Wolffian duct development. Sex Dev 2014; 8(5):273–280. doi: 10.1159/000363432. [PubMed: 24942390]
30. Schultheiss TM, James RG, Listopadova A, et al. Formation of the nephric duct In: The Kidney. From Normal Development to Congenital Disease. Academic Press; New York: 2003 pp. 51–60.
31. Breton S, Ruan YC, Park Y-J, et al. Regulation of epithelial function, differentiation, and remodeling in the epididymis. Asian J Androl 2016; 18(1):3–9. doi:10.4103/1008-682X.165946. [PubMed: 26585699]
32. Ridgeway AG, Petropoulos H, Wilton S, et al. Wnt signaling regulates the function of MyoD and myogenin. J Biol Chem. 2000; 275(42):32398–405. doi: 10.1074/jbc.M004349200 [PubMed: 10915791]
33. Pierucci-Alves F and Schultz BD. Bradykinin-stimulated cyclooxygenase activity stimulates vas deferens epithelial anion secretion in vitro in swine and humans. Biol Reprod 2008; 79(3): 501–509. doi: 10.1095/biolreprod.107.066910. [PubMed: 18480467]
34. Ye S, Zhang D, Cheng F, et al. Wnt/ -catenin β and LIF–Stat3 signaling pathways converge on Sp5 to promote mouse embryonic stem cell self-renewal. J Cell Sci. 2016; 129(2):269–276. doi: 10.1242/jcs.177675 [PubMed: 26598557]
35. Kennedy MW, Chalamalasetty RB, Thomas S, et al. Sp5 and Sp8 recruit β-catenin and Tcf1-Lef1 to select enhancers to activate Wnt target gene transcription. Proc Natl Acad Sci USA 2016; 113(13):3545–50. doi: 10.1073/pnas.1519994113. [PubMed: 26969725]
36. Jouneau A, Ciaudo C, Sismeiro O, et al. Naïve and primed murine pluripotent stem cells have distinct miRNA expression profiles. RNA 2012; 18(2):253–64. doi: 10.1261/rna.028878.111. [PubMed: 22201644]
37. Hirashima T Pattern formation of an epithelial tubule by mechanical instability during epididymal development. Cell Rep 2014; 9(3):866–873. doi: 10.1016/j.celrep.2014.09.041. [PubMed: 25437543]
38. Vandebrouck C, Melin P, Norez C, et al. Evidence that CFTR is expressed in rat tracheal smooth muscle cells and contributes to bronchodilation. Respir Res 2006; 7(1):113. doi: 10.1186/1465-9921-7-113 [PubMed: 16938132]
39. Cook DP, Rector MV, Bouzek DC, et al. Cystic fibrosis transmembrane conductance regulator in sarcoplasmic reticulum of airway smooth muscle. Implications for airway contractility. Am J Respir Crit Care Med 2016; 193(4):417–26. doi: 10.1164/rccm.201508-1562OC. [PubMed: 26488271]

Author Manuscript Author Manuscript Author Manuscript Author Manuscript

40. Risse PA, Kachmar L, Matusosky OS, et al. Ileal smooth muscle dysfunction and remodeling in cystic fibrosis. Am J Physiol Gastrointest Liver Physiol 2012; 303(1):G1–G8. doi: 10.1152/ajpgi.00356.2011. [PubMed: 22538405]
41. Sun H, Harris WT, Kortyka S, et al. TGF- β downregulation of distinct chloride channels in cystic fibrosis-affected epithelia. PLoS One 2014; 9(9):e106842. doi: 10.1371/journal.pone.0106842. [PubMed: 25268501]
42. Howe KL, Wang A, Hunter MM, et al. TGFβ down-regulation of the CFTR: a means to limit epithelial chloride secretion. Exp Cell Res 2004; 298:473–484. doi: 10.1016/j.yexcr.2004.04.026 [PubMed: 15265695]
43. Snodgrass SM, Cihil KM, Cornuet PK, et al. Tgf-β1 inhibits Cftr biogenesis and prevents functional rescue of ΔF508-Cftr in primary differentiated human bronchial epithelial cells. PLoS One 2013; 8(5):e63167. doi: 10.1371/journal.pone.0063167. [PubMed: 23671668]
44. Harris WT, Muhlebach MS, Oster RA, et al. Plasma TGF-β_1 in pediatric cystic fibrosis: potential biomarker of lung disease and response to therapy. Pediatr Pulmonol 2011; 46(7):688–95. doi: 10.1002/ppul.21430. [PubMed: 21337732]
45. Knowles MR, Drumm M. The influence of genetics on cystic fibrosis phenotypes. Cold Spring Harb Perspect Med 2012; 2(12):a009548. doi: 10.1101/cshperspect.a009548. [PubMed: 23209180]
46. Havasi V, Rowe SM, Kolettis PN, et al. Association of cystic fibrosis genetic modifiers with congenital bilateral absence of the vas deferens. Fertil Steril 2010; 94(6):2122–7. doi: 10.1016/j.fertnstert.2009.11.044. [PubMed: 20100616]
47. Kirk KL. CFTR channels and wound healing. Focus on “Cystic fibrosis transmembrane conductance regulator is involved in airway epithelial wound repair”. Am J Physiol Cell Physiol 201; 299(5):C888–890. doi: 10.1152/ajpcell.00313.2010.
48. Peitzman ER, Zaidman NA, Maniak PJ, et al. Agonist binding to β-adrenergic receptors on human airway epithelial cells inhibits migration and wound repair. Am J Physiol Cell Physiol 2015; 309(12):C847–855. doi: 10.1152/ajpcell.00159.2015. [PubMed: 26491049]
49. Chen J, Chen Y, Chen Y, et al. Epidermal CFTR suppresses MAPK/NF-kB to promote cutaneous wound healing. Cell Physiol Biochem 2016; 39(6):2262–2274. doi: 10.1159/000447919. [PubMed: 27832634]
50. Adam D, Bilodea C, Sognigbé L, et al. CFTR rescue with VX-809 and VX-770 favors the repair of primary airway epithelial cell cultures from patients with class II mutations in the presence of Pseudomonas aeruginosa exoproducts. J Cyst Fibros 2018; pii:S15690-1993(18) 30082–1. doi: 10.1016/j.jcf.2018.03.010.

Author Manuscript Author Manuscript Author Manuscript Author Manuscript

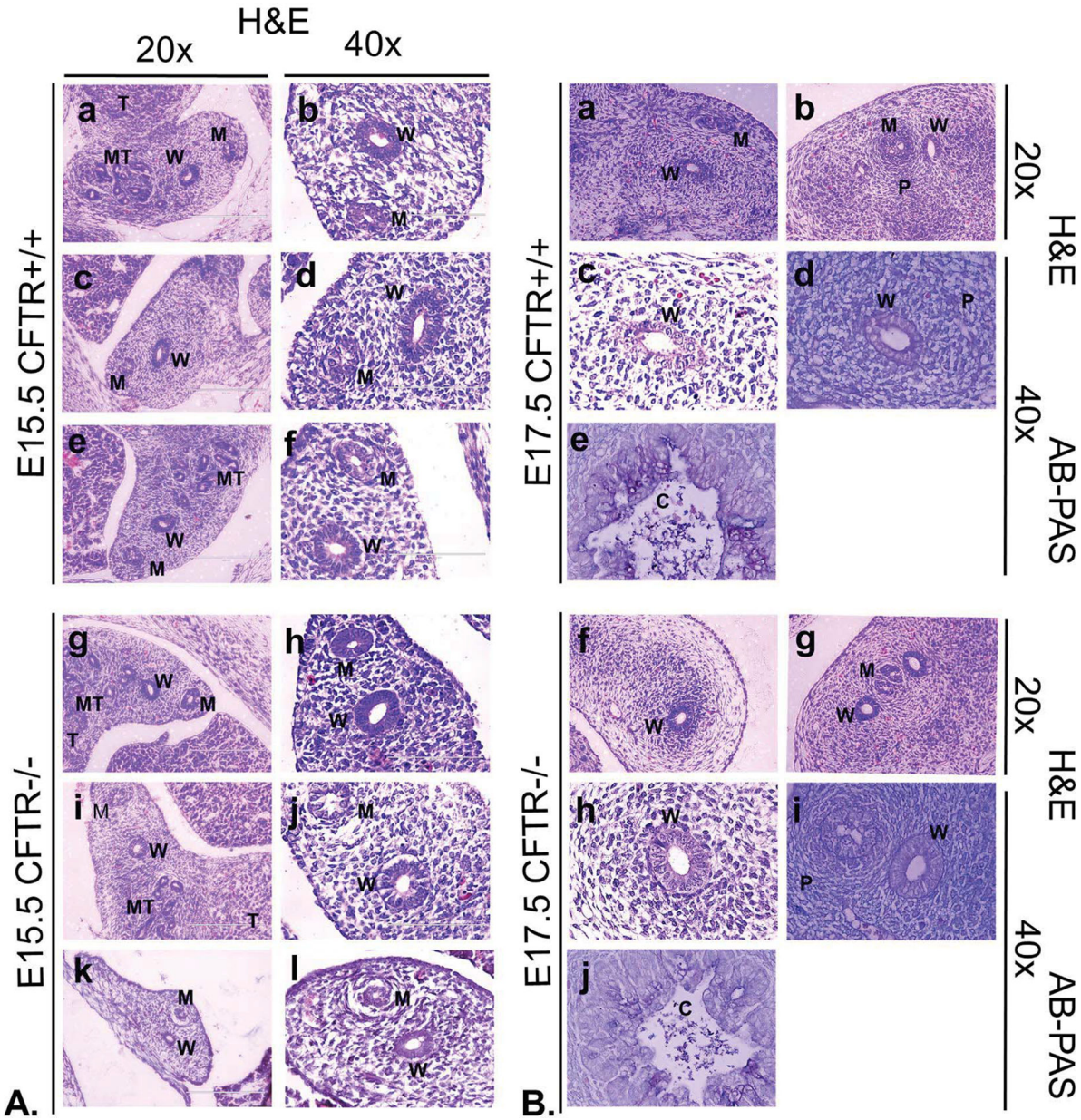

Figure 1: CFTR−/− male rat embryonic Wolffian and Mullerian duct formation is similar to wild type.

(Panel A) Wolffian and Mullerian ducts are patent in all sections and similar in appearance at E15.5 between corresponding wild type (a-f; N=3 animals) and CFTR−/− animals (g-l; N=4). Representative images are shown for the cranial region of the developing reproductive tract. In k and l, a CFTR−/− animal exhibits early signs of Mullerian duct regression. This timing is consistent with activity of anti-Mullerian hormone, which is secreted by Sertoli cells during a critical developmental window, E14.5-E16.5. (Panel B) Wolffian duct is patent in wild type (a-d) and CFTR−/− (f-i) male rat embryos at E17.5. Cranial Mullerian duct regression is suggested at this time point by apparent remnants of the embryonic structure (a). Panel B, images d, e, i, and j are stained with AB-PAS. All other sections are stained with H&E. AB-PAS of colon cross sections (Panel B; e, j) demonstrate mucin detection. W:

Wolffian, M: Mullerian, MT: mesonephric tubules, T: testis, P: region of developing prostate, C: colonic lumen.

Author Manuscript Author Manuscript Author Manuscript Author Manuscript

Author Manuscript Author Manuscript Author Manuscript Author Manuscript

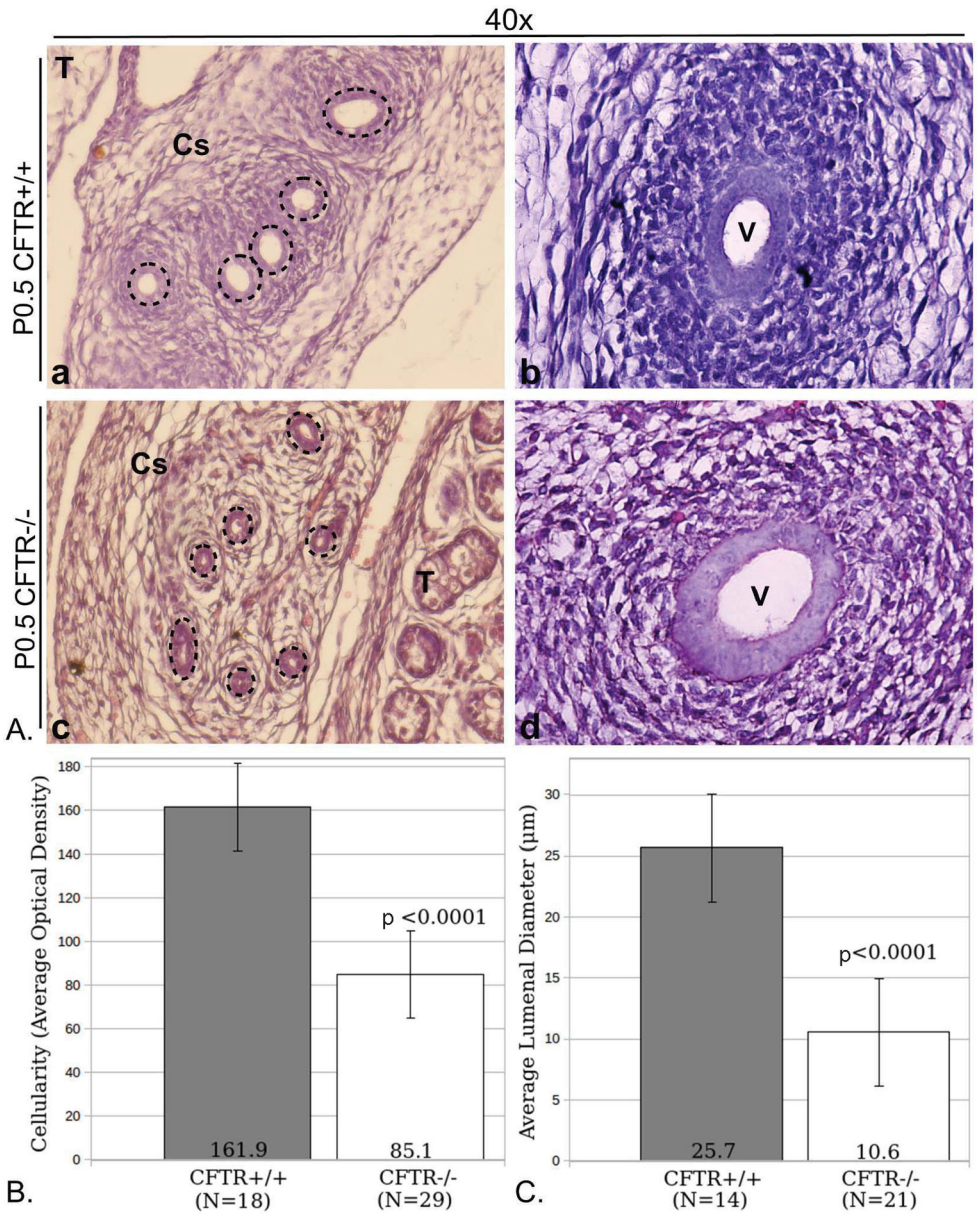

Figure 2: Reproductive duct abnormalities in newborn CFTR−/− male rats.

(Panel A) Typical reproductive tract morphology shown for CFTR+/+ (a,b) and CFTR−/− (c,d) tissues harvested at P0.5. Images are representative of observations from four wt and six CFTR−/− animals. Depicted are corpus epididymis (a, c) and vas deferens (b, d). Tissues from CFTR−/− animals demonstrate lessened mesenchymal cellularity (region immediately extrinsic to dashed circles) and decreased lumenal diameter of the corpus epididymis (c). Vas deferens with an obvious lumen could be observed regionally in all CFTR−/− samples investigated (d; see also Figure 3). Dashed lines (a, c) circumscribe epithelial cells that form the duct. (Panel B) ImageJ analysis of optical density showing reduced cellularity external to epithelial duct. Cellular densities immediately surrounding 18 CFTR+/+ and 29 CFTR−/− ducts were measured. (Panel C) reduced lumenal diameter in the corpus epididymis of CFTR−/− rats at birth. To obtain duct diameter, cross-sections from 14 CFTR+/+ and 21

CFTR−/− ducts were evaluated. Multiple sections from N=3 animals studied per group in Panels B and C; Error bars=SEM. T: testis, V: vas deferens, Cs: corpus epididymis.

Author Manuscript Author Manuscript Author Manuscript Author Manuscript

Author Manuscript Author Manuscript Author Manuscript Author Manuscript

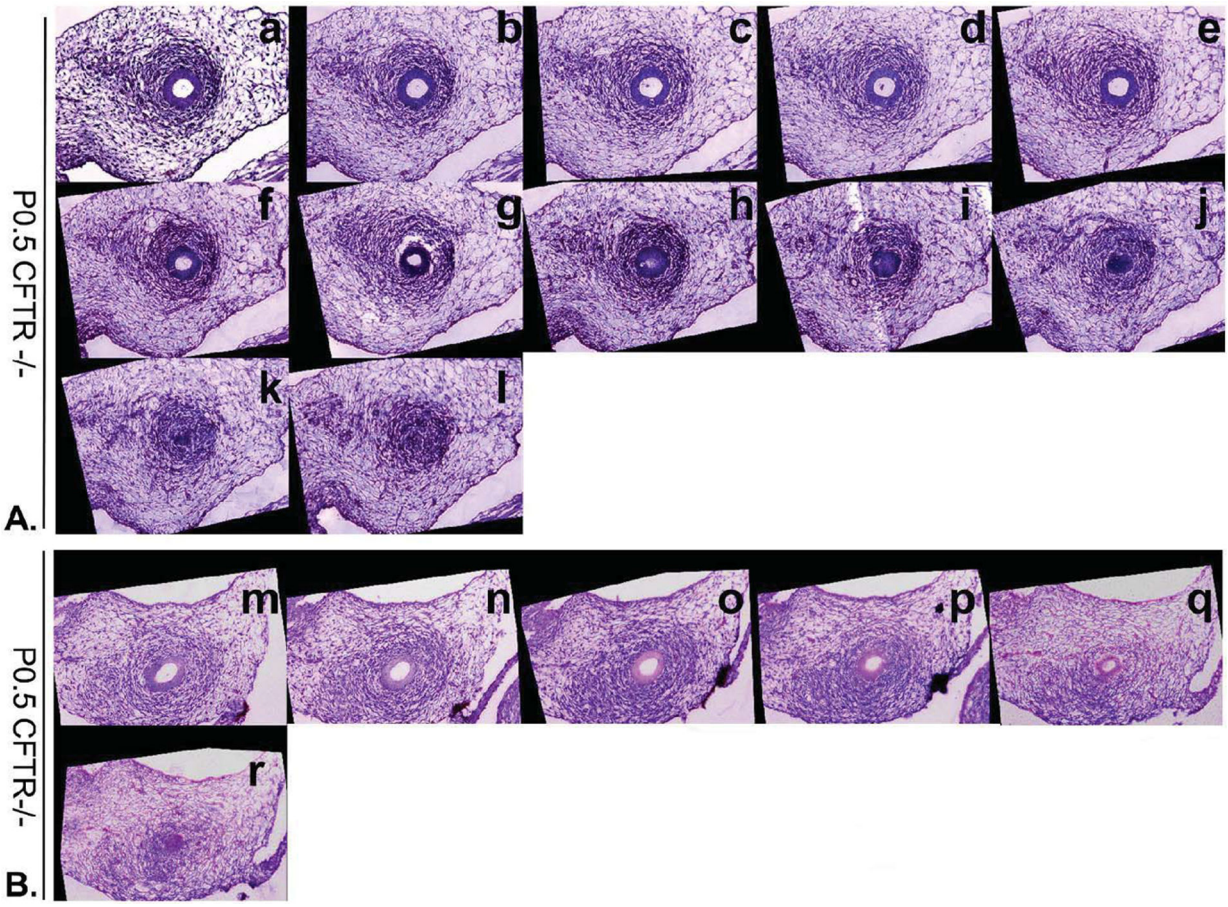

Figure 3: Evidence for perinatal collapse of CFTR−/− vas deferens by serial alignment of sections.

Images shown are arranged from proximal to distal at descending levels over 30–60 μm (5 μm increments). (Panel A) Sections stained with H&E demonstrate developing smooth muscle that encompasses a patent duct (a-e). Sections f, g and h show lumen aperture decreasing with no evidence of lumen in section i. Cells with epithelioid morphology are present in sections i and j, but not in sections k or l. (B) Comparable vas deferens observations in tissues from a second newborn CFTR−/− rat. All images are at 20x.

Author Manuscript Author Manuscript Author Manuscript Author Manuscript

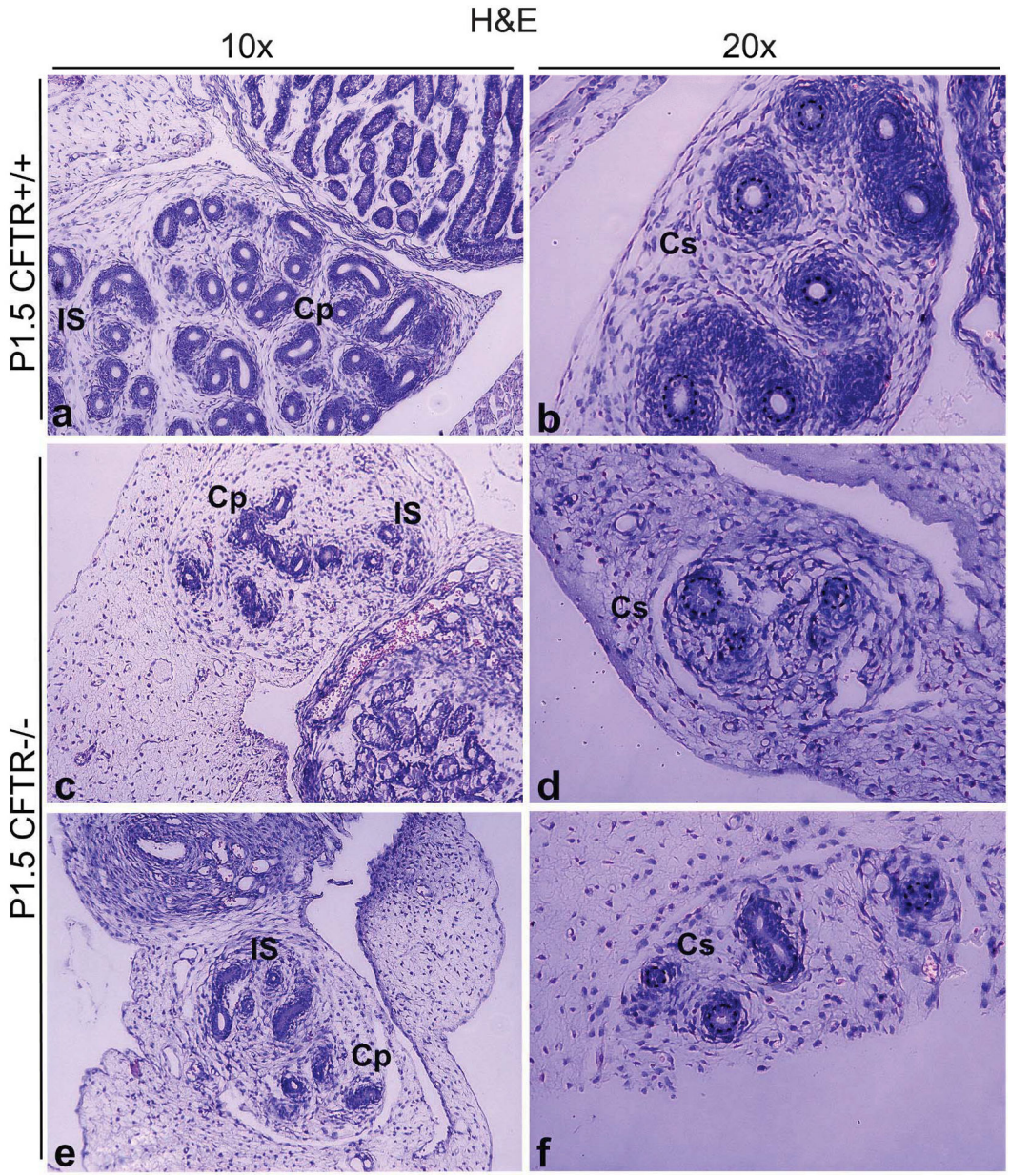

Figure 4: Under-development of epididymal regions in CFTR−/− male reproductive tract observed within the first two days of post-natal life.

CFTR+/+ (top row, representative images from N=3 animals) and CFTR−/− (bottom two rows, representing N=5 animals) sections at the level of initial segment/caput epididymis (a,c,e) and corpus epididymis (b,d,f). Note reduction of epididymal coiling, reduced luminal diameter, and diminished number and density of smooth muscle cells surrounding ducts (area immediately external to dashed circles, panels b, d & f) in CFTR−/− animals, particularly within the corpus epididymis. AB-PAS staining revealed no evidence of mucus obstruction in ducts of CFTR−/− rats (not shown). Cp: caput epididymis, Cs: corpus epididymis, IS: initial segment

Author Manuscript Author Manuscript Author Manuscript Author Manuscript

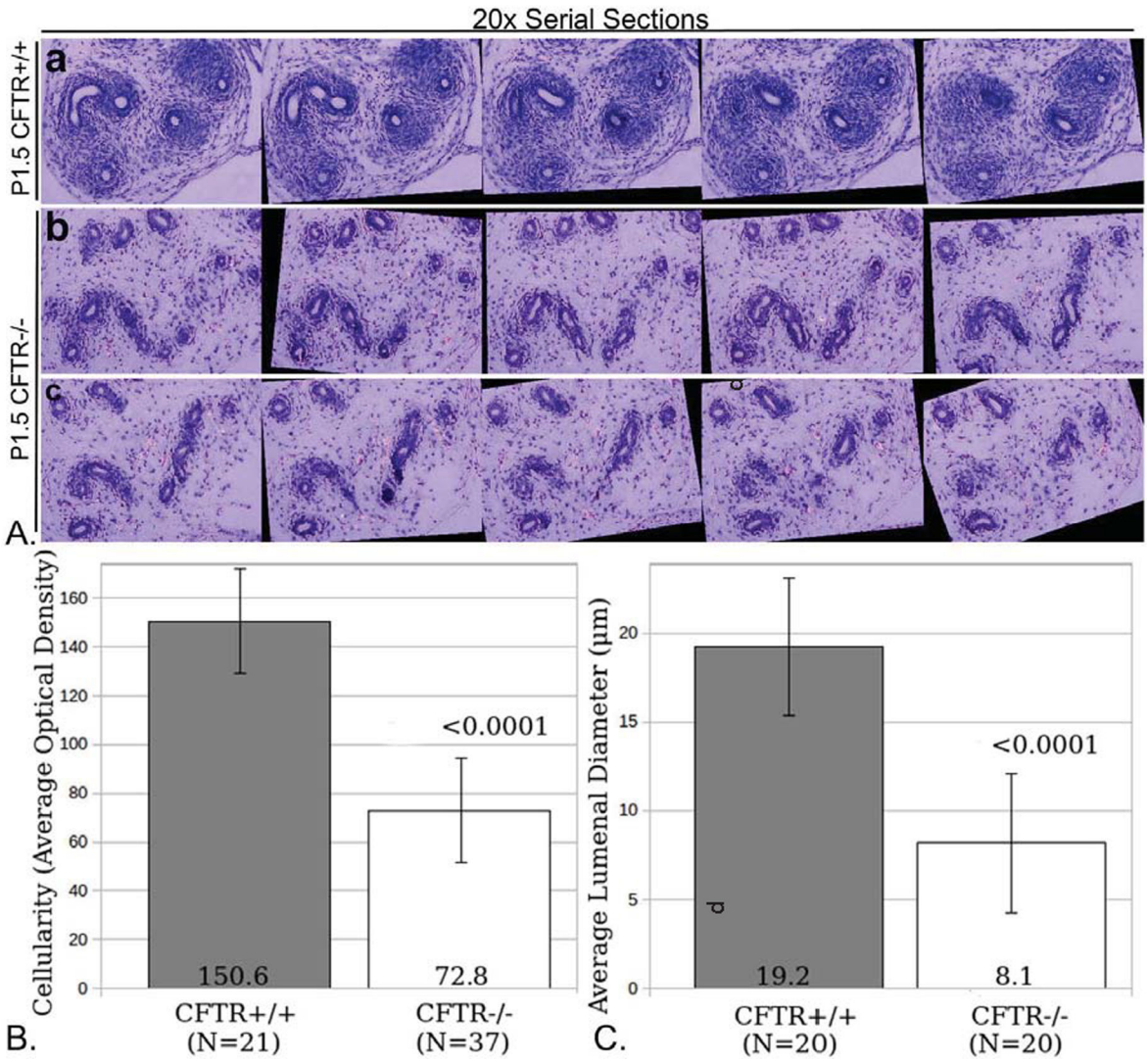

Figure 5: Reduced cellularity and luminal diameter of caput epididymis in two-day-old CF rat.

(Panel A) Serial sections from caput epididymis of CFTR+/+ (a) or CFTR−/− (b,c) animals were stacked and aligned using ImageJ (Methods) to visualize abnormal development of CFTR−/− epididymis. Note lack of smooth muscle proliferation surrounding CFTR−/− caput epididymal ducts (see also Figure 7). (Panel B) ImageJ analysis of optical density (O.D.) showing reduced cellularity external to epithelial duct. Cellular densities immediately surrounding 21 wild type and 37 CFTR null ducts were measured. (Panel C) Reduced lumenal diameter was observed in the caput epididymis of CFTR−/− rats at birth. To obtain duct diameter, 20 wild type and 20 CF ducts were evaluated (from 3 animals per group). Error bars= SEM.

Author Manuscript Author Manuscript Author Manuscript Author Manuscript

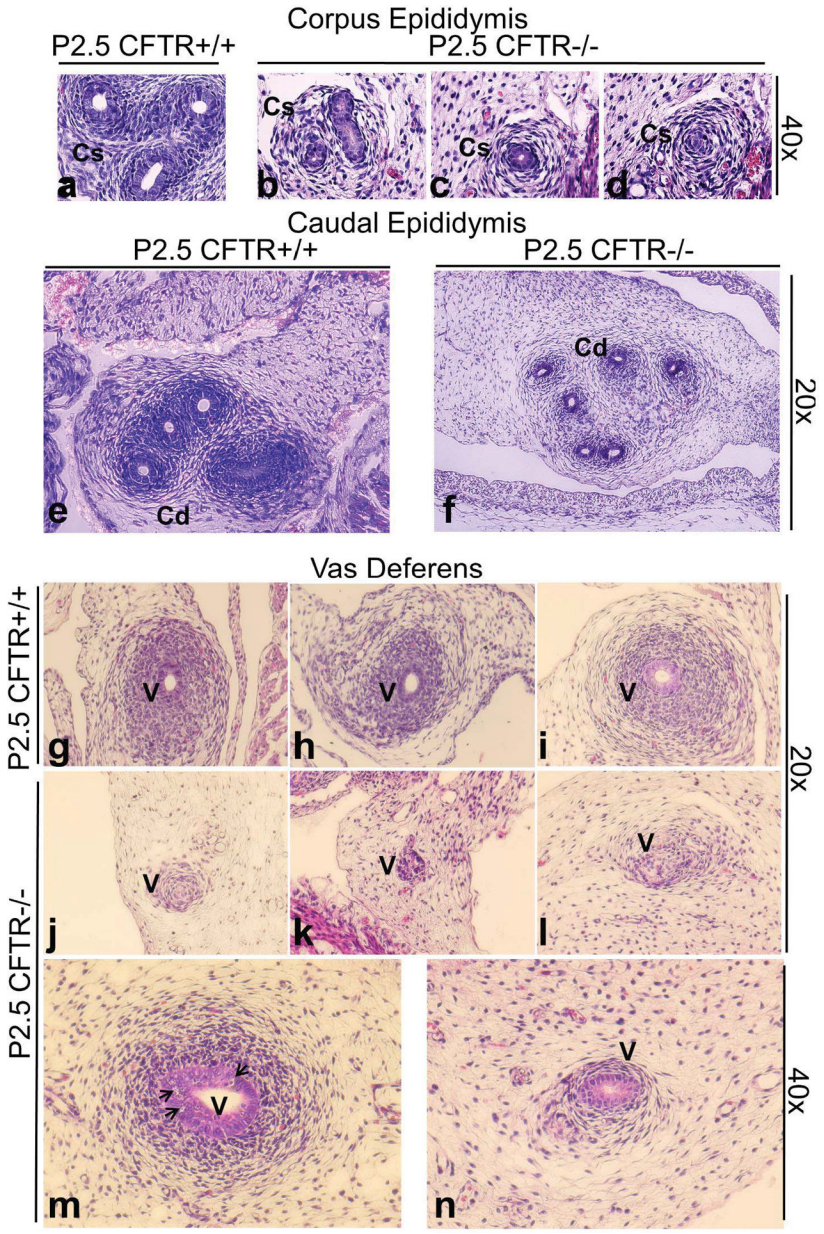

Figure 6: Epididymal abnormalities and ductular collapse, with degenerating vas deferens in 2–3 day old CFTR−/− male rats.

CFTR−/− animals at P2.5 (N=4) exhibit reduction in epididymis ranging from collapsed ducts (b-d) to general underdevelopment and reduced cellularity (f) in comparison to wild type (a,e). Wild type vasa deferentia are shown in g-i with patent lumen and developing mesenchyme. Vas deferens remnants typically were observed at P2.5 in CFTR−/− rats (j-l). Occasionally a lumen was observed (m), but serial sections showed that the lumen was reduced and became absent in more distal regions (n), accompanied by markedly reduced mesenchymal cell proliferation. Vacuolation (suggestive of degenerating cells) was observed within vas epithelia (m, arrows) Cs: corpus epididymis, Cd: cauda epididymis, V: vas deferens

Author Manuscript Author Manuscript Author Manuscript Author Manuscript

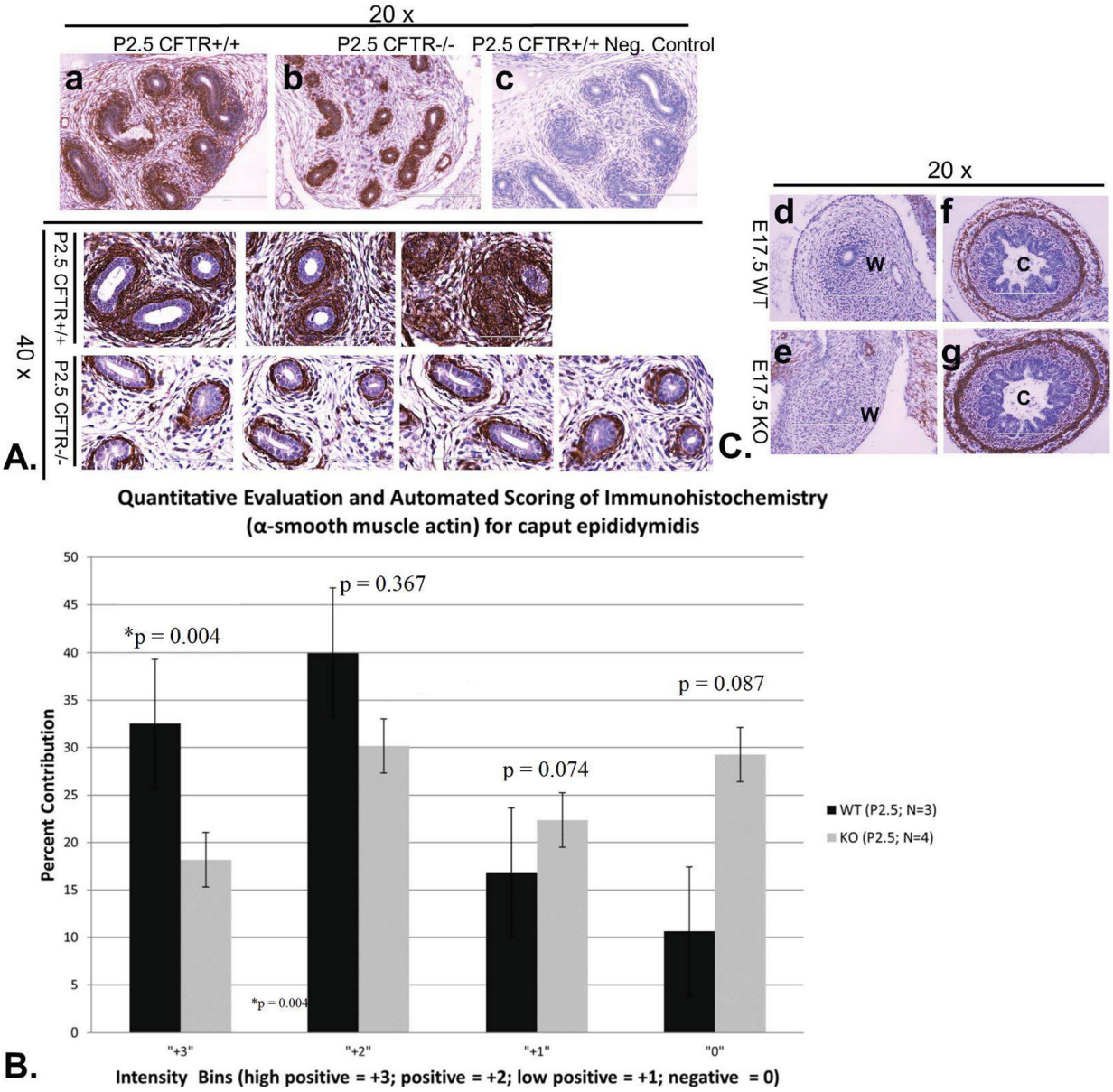

Figure 7: Abnormal smooth muscle development in caput epididymis of CFTR−/− animals.

(Panel A) α-SMA labeling (top row; hematoxylin counterstain) of CFTR+/+ (a) and CFTR −/− (b) caput epididymis (20x view). No labeling was observed when primary antibody was omitted from the protocol (c). Replicate labeling (lower two rows) is shown for α-SMA in caput epididymes of P2.5 CFTR+/+ or CFTR−/− animals (40x view, representative of 3–4 animals per condition). (Panel B) IHC Profiler (ImageJ) quantification of 3,3′-diaminobenzidine (DAB) stained α-SMA. Note that a higher proportion of CFTR+/+ ducts exhibit high intensity labeling (+3 & +2) whereas the distribution of intensity for ducts from knockout (KO) animals is more evenly distributed. (Panel C) α-SMA immunolabeling of E17.5 Wolffian (mesonephric) duct (d,e) or colonic tissue (f,g) otherwise studied as in Panel A. Note lack of α-SMA surrounding the reproductive tract in both wildtype and CFTR−/−

Author Manuscript Author Manuscript Author Manuscript Author Manuscript

animals at a time point when no abnormality is observable in this region of the CFTR−/− fetus. C: colon, W: Wolffian duct

Author Manuscript Author Manuscript Author Manuscript Author Manuscript

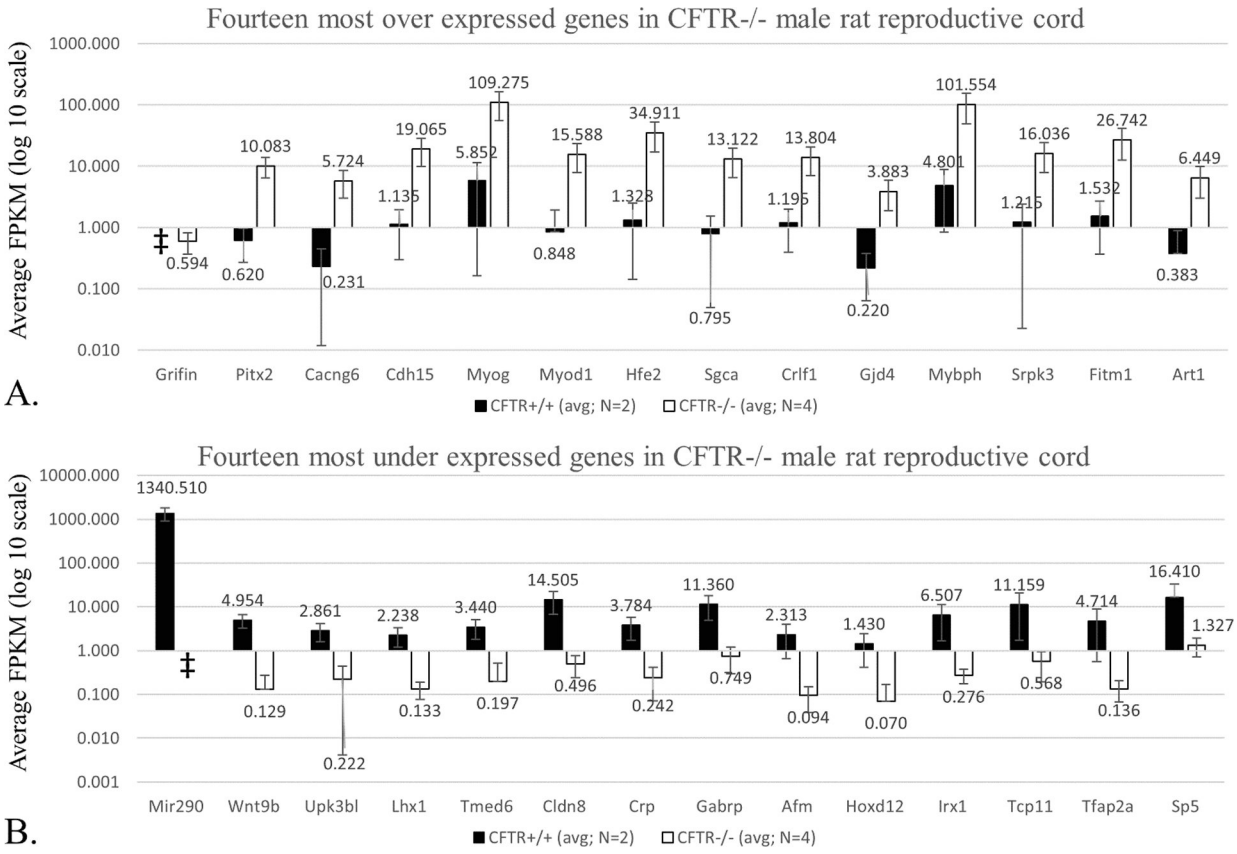

Figure 8: RNA-seq analysis reveals over- (A) and under- (B) expressed transcripts in CFTR−/− male reproductive cord at birth.

Graphical representation of FPKM (fragments per kilobase transcript per million fragments) for CFTR+/+ and CFTR−/− using epididymis, vas deferens, and surrounding tissue as source of mRNA. Complete dataset is shown in Supplemental Table 1. y-axis = log 10 scale; ‡ indicates FPKM value = 0, and not represented in this data format.

Author Manuscript Author Manuscript Author Manuscript Author Manuscript

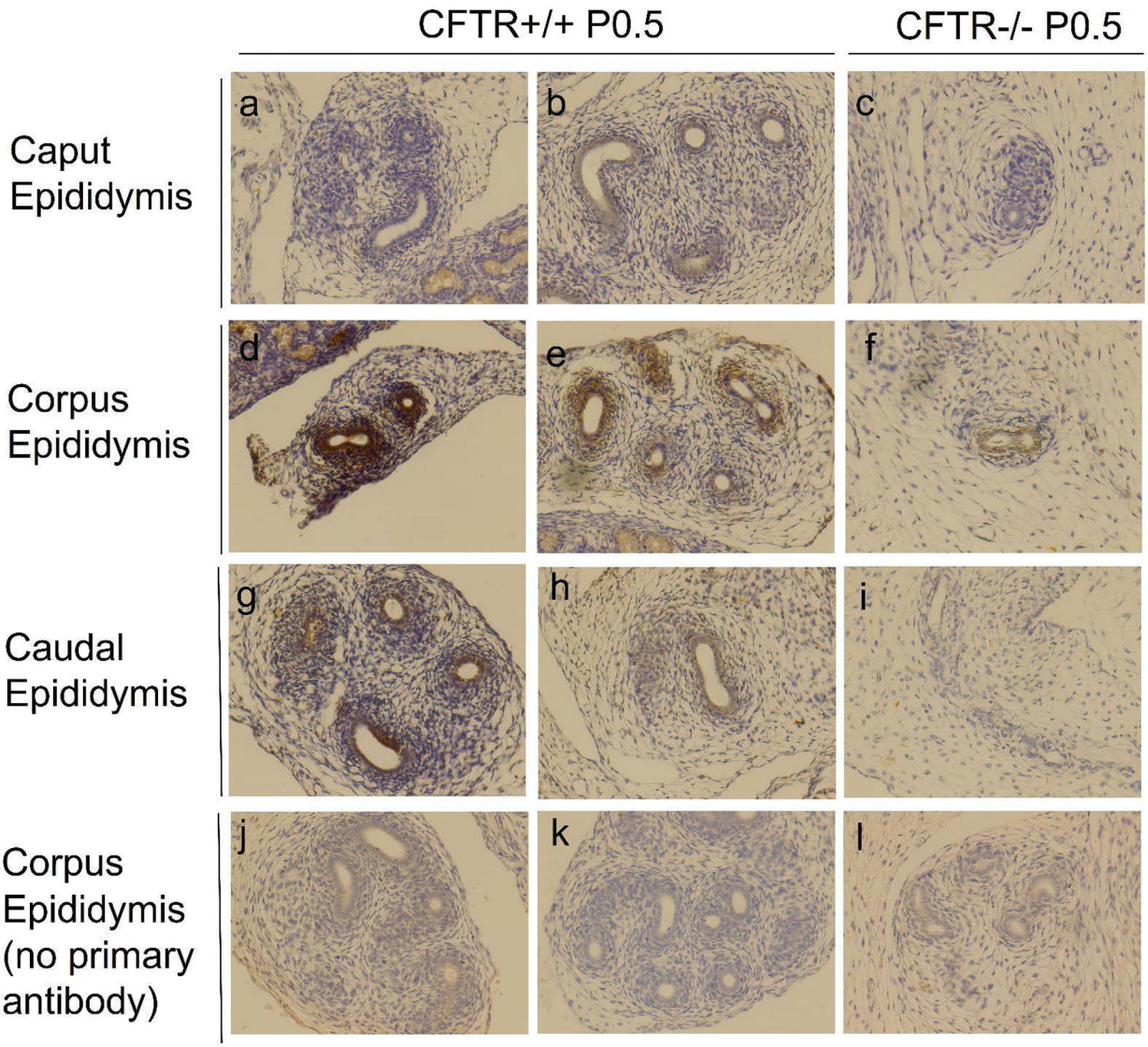

Figure 9: Wnt9b expression is reduced in CFTR−/− epididymis.

Immunolabeling for Wnt9b expression within (a-c) caput, (d-f) corpus, and (g-i) cauda epididymis in CFTR+/+ (left and middle columns; representative sections from N=2 animals) and CFTR−/− (right column; N=2) at P0.5 (birth). Regional variation in Wnt9b immunolabeling is observed with the most intense signal generated in corpus epididymis for both CFTR−/− and CFTR+/+ rats. Controls without primary antibody are also shown (j-l). Images taken at 20x.

Author Manuscript Author Manuscript Author Manuscript Author Manuscript

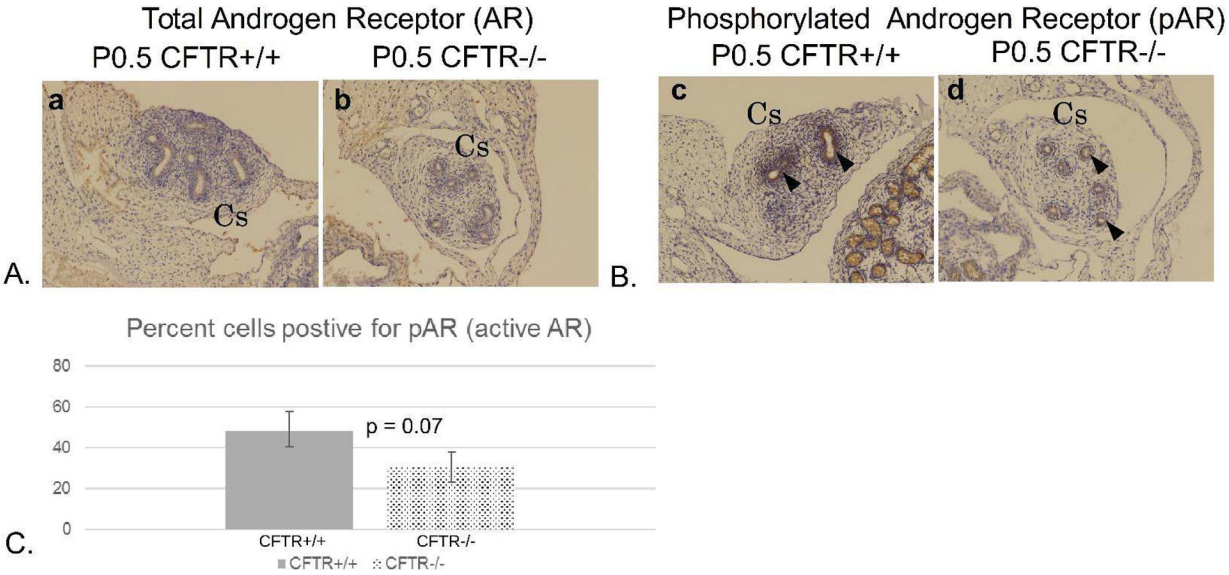

Figure 10: Androgen receptor (AR) phosphorylation is reduced in corpus epididymis of CFTR−/− rats.

(Panel A) Total AR labeling appears comparable between newborn CFTR+/+ and CFTR−/− samples, (Panel B) The level of phosphorylated AR (antibody detects residues S210/S213) was less in epithelial cells lining the CFTR−/− duct, particularly in the region of the corpus epididymis (arrow heads). (Panel C) Quantitation showing % cells positive for activated AR. Cs: corpus epididymis

Author Manuscript Author Manuscript Author Manuscript Author Manuscript

Table 1:

Statistically over-represented biological processes, molecular functions, and signaling pathways for transcripts altered in CF reproductive tract.

PANTHER GO-Slim Biological Process	**Total in *Rattus norvegicus* (of 23781)**	**Expected out of 72**	**No. out of 72 significantly altered**	**Fold Enrichment**	**P-value (Bonferoni corrected)**
Muscle organ development (GO: 0007517)	250	0.74	8	10.87	0.00019
Developmental process (GO:0032502)	1951	5.74	19	3.31	0.000582
Ectoderm development (GO:0007398)	399	1.17	9	7.66	0.000656
System development (GO:0048731)	1051	3.09	13	4.2	0.00262
Muscle contraction (GO:0006936)	158	0.47	5	10.75	0.0264
Nervous system development (GO: 0007399)	667	1.96	9	4.58	0.0359
Protein ADP-ribosylation (GO:0006471)	6	0.02	2	> 100	0.0366
PANTHER GO-Slim Molecular Function	**Total in *Rattus norvegicus* (of 23781)**	**Expected out of 72**	**No. out of 72 significantly altered**	**Fold Enrichment**	**P-value (Bonferoni corrected)**
Sequence-specific DNA binding transcription factor activity (GO: 0003700)	1263	3.72	14	3.77	0.00286
DNA binding (GO:0003677)	1542	4.54	14	3.08	0.0247
PANTHER Pathways	**Total in *Rattus norvegicus* (of 23781)**	**Expected out of 72**	**No. out of 72 significantly altered**	**Fold Enrichment**	**P-value***
Histidine biosynthesis (P02747)	2	0.01	1	> 100	0.00587
Cadherin signaling pathway (P00012)	151	0.44	3	6.75	0.0102
Wnt signaling pathway (P00057)	314	0.92	4	4.33	0.014
Gamma-aminobutyric acid synthesis (P04384)	6	0.02	1	56.62	0.0175
Vitamin D metabolism and pathway (P04396)	16	0.05	1	21.23	0.046

* p-values for “PANTHER Pathways” not Bonferoni corrected due to the large number of tests performed.